The AAPM/RSNA Physics Tutorial for Residents

CME FEATURE

This article meets the criteria for 1.0 credit hour in Category 1 of the AMA Physician's Recognition Award. To obtain credit, see the questionnaire on pp 439-442.

An Introduction to MR Angiography[1]

David Saloner, PhD

This article provides an overview of the basic principles of magnetic resonance (MR) angiography. The parameters in MR imaging manipulated to generate high contrast between flowing nuclei and stationary tissue are discussed. Two primary strategies are used: time-of-flight (TOF) MR angiography, which creates differences in magnetization magnitude between flowing and stationary nuclei, and phase-contrast MR angiography, which induces changes in the spatial orientation, or phase, of flowing nuclei relative to stationary nuclei. The end result of an MR angiographic study is typically a three-dimensional data set composed of either sequential two-dimensional sections or true three-dimensional data. Two-dimensional TOF methods are sensitive to slow flow and are valuable for differentiating between slow flow and occlusion. Three-dimensional TOF methods have better resolution and are more useful in imaging tortuous vessels. Phase-contrast MR angiography can be effectively used to avoid problems of magnetization saturation that occur in three-dimensional TOF studies and to eliminate signal from high-intensity stationary material such as blood products, which may appear bright and mimic flow signal in TOF studies. Careful use of postprocessing tools aids in the assessment of vascular abnormalities once the MR angiographic data have been acquired.

■ INTRODUCTION

The sensitivity of magnetic resonance (MR) imaging to moving nuclei has been appreciated from the earliest clinical studies with the modality. In recent years, there has been substantial progress in developing and evaluating techniques for assessing vascular pathologic conditions with MR imaging. Because these methods have similar goals to those of x-ray angiography and because the two modalities produce images that have many similar features, the MR imaging methods have been called MR angiography (1-5).

Abbreviations: GRE = gradient-recalled echo, MIP = maximum intensity projection, RF = radio frequency, TE = echo time, TOF = time of flight, TR = repetition time

Index terms: Magnetic resonance (MR), vascular studies, 9.12942 • Physics

RadioGraphics 1995; 15:453-465

[1] From the Department of Radiology (114), Veterans Administration Medical Center, University of California, San Francisco, 4150 Clement St, San Francisco, CA 94121. From the AAPM/RSNA Physics Tutorial at the 1993 RSNA scientific assembly. Received June 9, 1994; revision requested July 12 and received November 17; accepted December 6. **Address reprint requests to** the author.

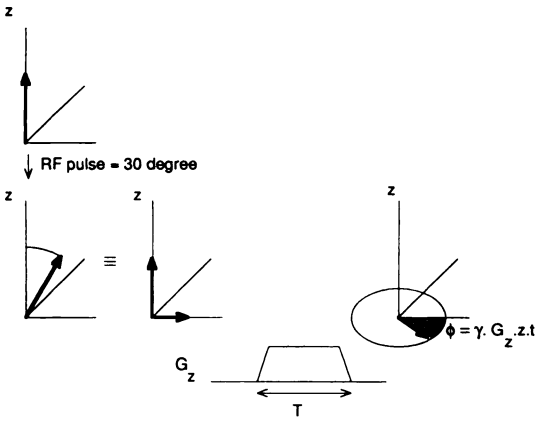

Figure 1. Diagram illustrates response of magnetization to RF pulse and imaging gradient. The RF pulse creates a component of transverse magnetization that is rotated around the longitudinal axis by the imaging gradient (G_z). Both the orientation (ϕ) and magnitude of the transverse magnetization can be measured. t = time that gradient has been applied, T = total duration of the gradient, γ = gyromagnetic ratio.

MR angiography is an attractive modality for evaluating vascular disease. Vessel accessibility is not a problem as it is with ultrasonography (US). Patients are spared the discomfort of and potential risk of adverse reactions from the injection of contrast material needed for conventional x-ray angiography.

This article examines the basic principles underlying the establishment of signal contrast between flowing and stationary nuclei. The fundamental approaches to the acquisition and display of vascular signal in MR angiography are discussed. Methods for improving image quality, such as appropriate selection of imaging parameters, careful application of postprocessing, application of presaturation bands, and implementation of flow compensation techniques, are reviewed.

■ X-RAY VERSUS MR ANGIOGRAPHY

The information contained in an MR angiogram is not identical to that contained in an x-ray angiogram, even though the two images may have very similar appearances. Conventional angiograms are produced by injecting contrast medium at a specific site in the vasculature and imaging the contrast material as it moves downstream from the injection site. Vessels are thus selectively displayed. Furthermore, the contrast material diffuses relatively rapidly through the full vessel volume, and the image signal strength reflects the intraluminal density of contrast material. The angiogram is acquired after the desired viewing angle is selected, and an image is created in projection onto that viewing plane.

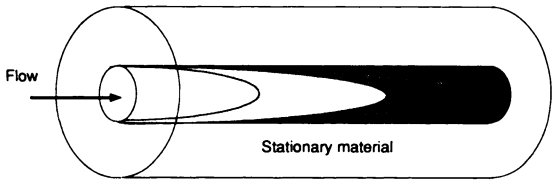

Figure 2. Drawing illustrates magnetization replenishment. Nuclei entering the imaging volume bring in unsaturated magnetization and receive one additional RF excitation for each additional TR interval that they remain in the excitation volume. The unshaded parabola represents "fresh" unsaturated magnetization. Regions that have received additional excitation are depicted with increasingly heavy shading.

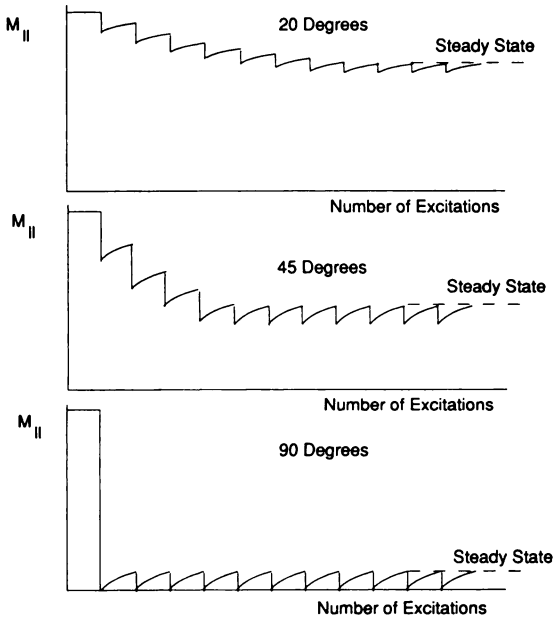

Figure 3. Plots depict the strength of the longitudinal magnetization of nuclei ($M_{||}$) as a function of the number of RF pulses received. The reduction in longitudinal magnetization with each pulse depends on the flip angle. The steady state is reached more quickly with larger flip angles.

MR angiograms are acquired by exciting nuclei in a selected volume of interest and detecting the signal contrast between all moving nuclei and stationary nuclei within that volume. In general, vessel depiction in MR angiography, unlike x-ray angiography, does not arise from a selective study. Although vascular signal strength in MR angiography is related to the proton density of blood, blood flow patterns play a pivotal role in the appearance of MR angiograms. Finally, in most MR imaging techniques, an explicit three-dimensional data set is collected.

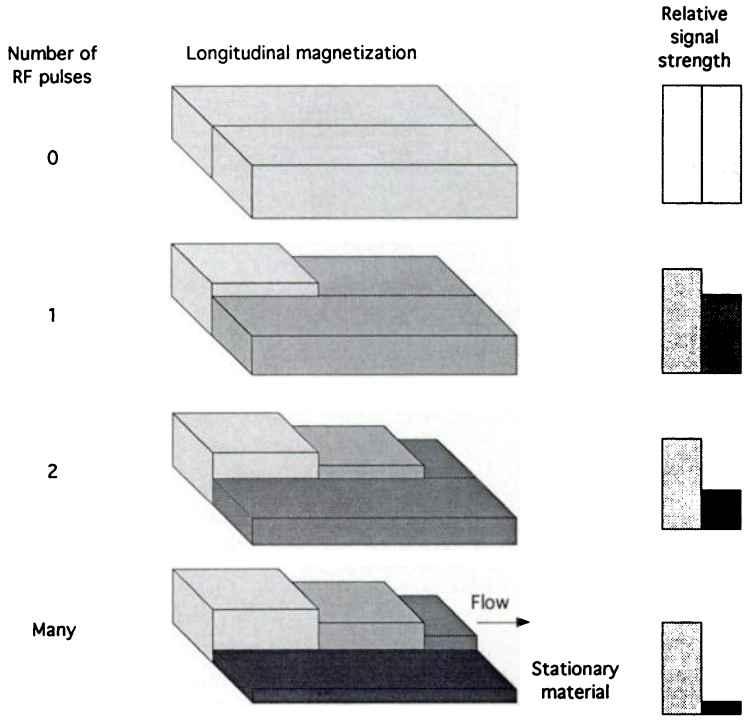

Figure 4. Progression of longitudinal magnetization to steady state for flowing nuclei and stationary material is shown as the two different volumes are subjected to an increasing number of RF pulses. The "longitudinal magnetization" column shows the strength of the longitudinal magnetization through the excited volume. The "relative signal strength" column shows the net signal from flowing nuclei (left bar) and stationary nuclei (right bar) and represents a sum over the thickness of the excited volume.

These data can be postprocessed to display views of the data in any number of viewing planes after the patient has left the imager.

■ SIGNAL CONTRAST IN MR ANGIOGRAPHY

In MR imaging, use of gradient-recalled echo (GRE) pulse sequences provides desirable contrast properties with short repetition times (TRs). Selectable radio-frequency (RF) flip angles provide additional control of image contrast properties. In a GRE sequence, the magnetization following the small RF excitation pulse can be represented as the longitudinal and transverse magnetization components. When the transverse magnetization is measured in MR imaging (and in particular in MR angiography), both the magnitude and orientation of the magnetization in the transverse plane can be determined (Fig 1). The orientation, referred to as the phase of the magnetization, will vary depending on the response of the nuclei to the applied magnetic field gradients.

Images that display the magnitude of the magnetization rely on inflow replenishment to create contrast between flowing blood and stationary tissue (Fig 2). They are referred to as time-of-flight (TOF) images. Images that display the phase of the magnetization rely on the motion of nuclei with respect to the imaging gradients for vessel-to-stationary tissue contrast. They are referred to as phase-contrast images. Stationary nuclei remain in the imaging section throughout the data acquisition interval and receive many RF excitations.

The strength of the longitudinal magnetization of nuclei subjected to a series of RF pulses decreases with each excitation (Fig 3). Between RF pulses, there is a small amount of relaxation that depends on the T1 of the material. The reduction in longitudinal magnetization with each pulse depends on the size of the excitation angle (ie, flip angle). After receiving a sufficient number of RF excitations, the material reaches a steady state in which the longitudinal magnetization removed is restored by longitudinal relaxation. Thus, the magnetization strength of stationary nuclei (ie, those nuclei that stay within the excitation volume for the entire acquisition period) decreases to the steady state value. Moving nuclei may receive only a few RF pulses and thus retain substantial magnetization strength.

Differences in longitudinal magnetization between stationary and flowing material become pronounced as nuclei within the imaging volume receive multiple RF pulses. The flowing nuclei receive a number of excitations that are limited by the section thickness and that decrease with increasing flow velocity. Freshly arriving nuclei bring unsaturated magnetization into the imaging volume. This results in high contrast between flowing and stationary nuclei (Fig 4).

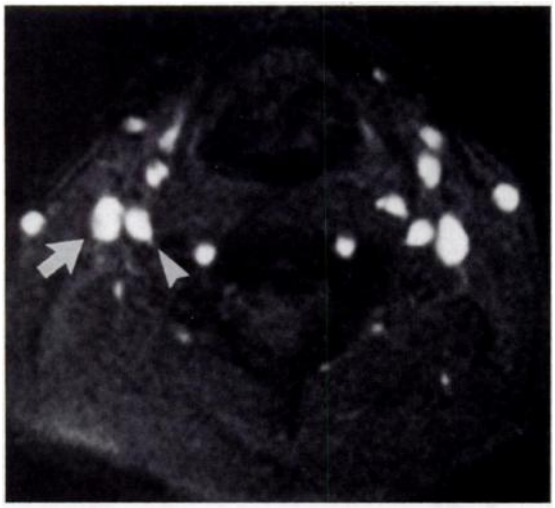

Figure 5. Axial MR image of the neck of a healthy volunteer shows both arteries and veins. A flow-compensated GRE pulse sequence with the following parameters was used: 40/10 (TR msec/echo time [TE] msec), 40° flip angle, 4-mm section thickness. Arrowhead = common carotid artery, arrow = jugular vein.

The high contrast between flowing and stationary nuclei in a two-dimensional single-section MR angiogram is seen in Figure 5. The signal from the stationary nuclei is strongly suppressed. Both arteries and veins can be seen, since high signal is acquired from flowing nuclei independent of flow direction in MR angiography.

The end result of an MR angiographic study is typically a three-dimensional data set composed of either sequential two-dimensional sections or true three-dimensional data. Because it is difficult to evaluate tortuous anatomy from individual sections alone, a projection image is produced by mapping the signal onto a desired viewing plane by means of a maximum intensity projection (MIP) algorithm. The MIP algorithm projects rays perpendicular to each pixel in the plane of the image through the MR angiographic data set (6). The highest intensity signal along each such ray is mapped onto the projection image (Fig 6). The MIP image can be generated in any desired viewing plane and provides a rapid overview of the overall geometry of the vasculature. However, because MIP images have associated artifacts, suspected pathologic entities should be confirmed on the source images.

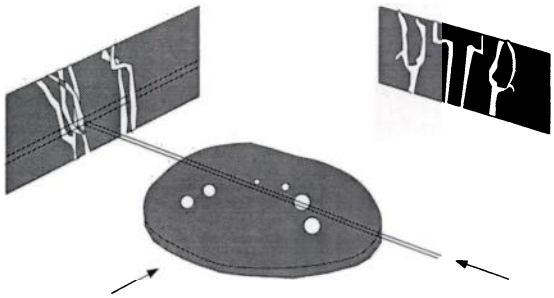

Figure 6. Drawing illustrates the implementation of the MIP algorithm. Rays are projected perpendicular to each pixel in the plane of the desired image through the MR angiographic data set. The highest intensity signal along each ray is mapped onto the projection image.

Postprocessing artifacts can be reduced by limiting the volume of data that is to be included in the postprocessing step. In this approach, the user defines a restricted volume in the full data set on which postprocessing is performed. The contribution of random fluctuations in signal from the stationary nuclei and vessel overlap can be reduced in this way. This technique is illustrated for an MR angiogram of the carotid artery bifurcation (Fig 7).

In an MR angiographic study composed of sequential two-dimensional sections, the high signal from closely neighboring arteries and veins can confuse the interpretation of images. Presaturation pulses (or bands) can be used to eliminate flow signal originating from one side of the imaging volume. Use of an additional RF pulse placed on one side of the imaging volume will suppress the magnetization strength of flowing blood before it enters the imaging volume (Fig 8). The vessel will thus be eliminated in image sections acquired downstream from the presaturation slab. Arteries or veins can then be selectively imaged. This strategy can also be used to identify flow directionality or to identify vessels feeding a specific territory (7). In some situations, a presaturation band is used that remains fixed in space for the total acquisition. In other cases, typically in two-dimensional studies, the presaturation band keeps a fixed distance from the imaging section and therefore "travels" or "walks" along with it (Fig 9). The gap between the presaturation band and the imaging section can also be varied. In some applications, the presaturation band can even be placed to partially overlap the imaging

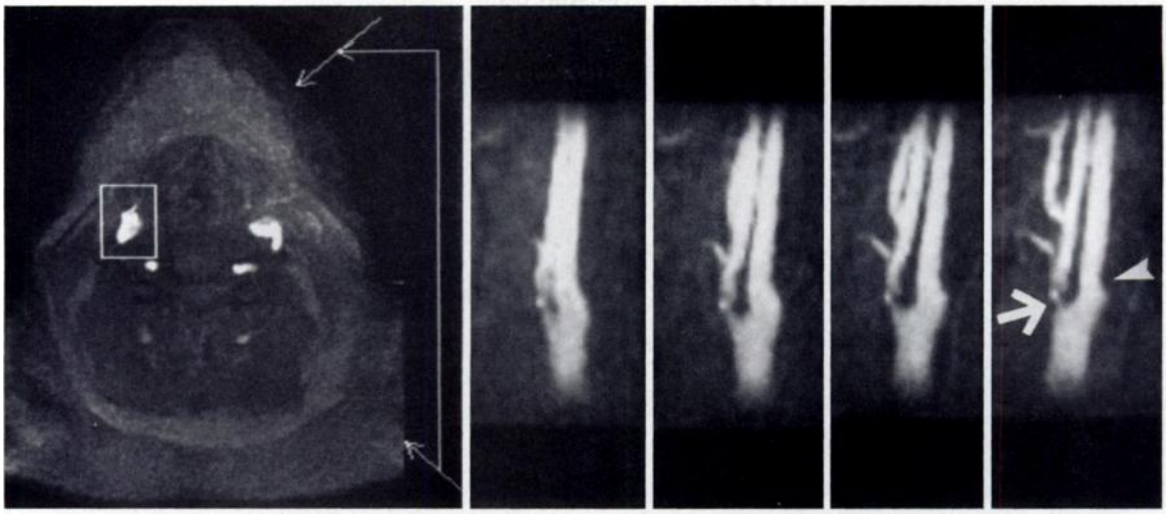

Figure 7. Defining the volume of image data for postprocessing. Image on the far left is an MIP in the transverse plane from a three-dimensional MR angiographic acquisition (40/7, 52-mm-thick slab, 64 partitions) through the carotid artery bifurcation. The volume selected for postprocessing is outlined by the rectangle, and the range is indicated by the arrows. MIP images of the selected volume over the right carotid bifurcation are shown in 25° increments around the head-foot axis. Stenosis of the external carotid artery (arrow) and the presence of moderate plaque in the internal carotid artery (arrowhead) are seen.

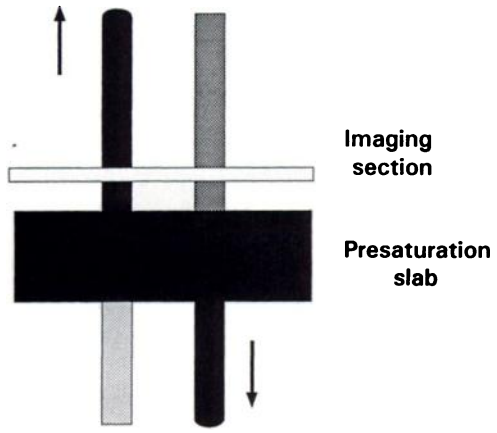

Figure 8. Diagram depicts placement of a presaturation pulse or slab. An RF pulse placed on one side of the imaging volume suppresses the magnetization strength of blood entering from below the imaging section.

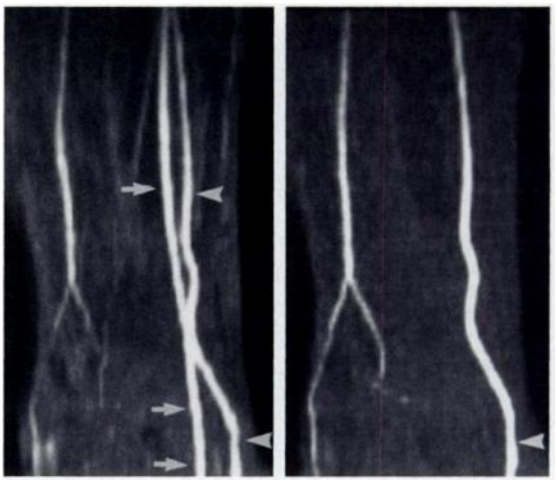

a. **b.**

Figure 9. Coronal MIP MR angiograms of a lower extremity demonstrate the effect of presaturation. Images were constructed from sequential axial two-dimensional sections (40/8, 45° flip angle, 3-mm section thickness) without saturation bands **(a)** and with the edge of a 40-mm presaturation slab placed 10 mm inferior to the imaging section **(b)**. The venous signal seen in **a** (arrows) is removed, and the arterial signal (arrowheads) is clearly identified.

section, thereby providing additional suppression of signal from stationary tissue.

Sequential two-dimensional MR angiographic studies have limited resolution in the direction of the section thickness and have relatively long TEs. MR angiographic studies composed of true three-dimensional data have improved resolu-

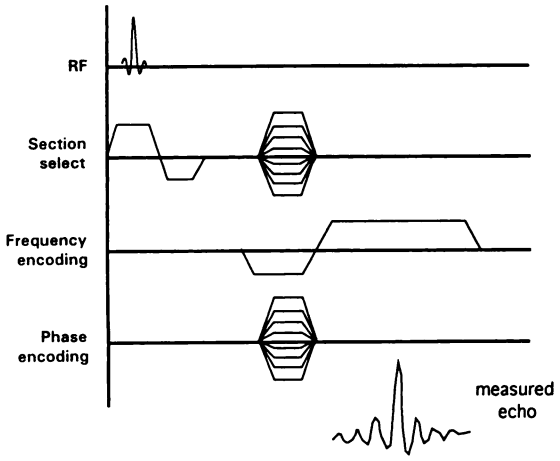

Figure 10. Diagram of a three-dimensional pulse sequence depicts a second loop of phase encoding being applied along the section-select axis.

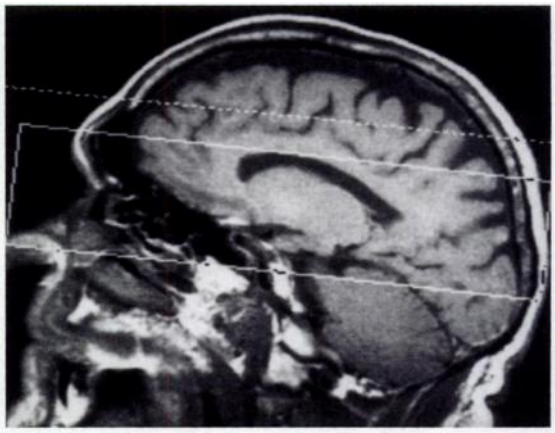

Figure 11. Sagittal MR scout view of the head illustrates the prescription of a three-dimensional MR angiographic study. This shows the use of a 52-mm-thick axial slab (solid line) rotated through a small angle toward the coronal plane to cover the circle of Willis. The inferior edge of a superior presaturation slab (dashed line), which has been placed to remove venous return, is also seen.

tion and reduced TEs (8). In the latter method, RF excitation is applied to a large slab (typically 50 mm thick), and a second loop of phase encoding is performed to partition the slab into many thin partitions (typically 0.7 mm thick) (Fig 10). The signal echo is acquired from the entire volume of excited material for each combination of phase-encoding steps. The three-dimensional pulse sequence is similar to the two-dimensional pulse sequence but differs in that the excited volume is a thick slab as opposed to a thin section and a second series of phase-encoding steps is performed along the slab-select direction. This technique serves to differentiate signals originating at different levels in the three-dimensional volume. The three-dimensional data set then consists of multiple two-dimensional partitions. A clinical example of a three-dimensional MR angiographic study is shown in Figure 11.

The choice of imaging parameters for three-dimensional MR angiography requires making a compromise between different objectives. In general, vessel-to-background contrast is increased by reducing background signal as much as possible. However, particularly for three-dimensional studies, nuclei may remain in the excitation volume and experience several RF pulses. Thus, parameter choices that decrease the signal from stationary nuclei may also decrease vessel-to-background contrast. This loss of contrast will be large in images obtained with large flip angles and short TRs, particularly in distal portions of the vessel. Blood has a variety of flow velocities, with the fastest streamline generally running down the center of the vessel. Signal loss occurs as the vessel courses distally into the imaging slab, with signal loss progressing from the edges of the lumen, where the blood flow is slowest, to the center of the vessel.

Suppression of signal from stationary material increases as flip angles increase. However, the high contrast from unsaturated magnetization in newly arriving flowing nuclei is more rapidly lost with increasing flip angle. A compromise must be made between the two limits. The effect of flip angle choice on image contrast can be seen in lateral MIP images from three-dimensional MR angiographic studies of the carotid bifurcation (Fig 12).

The effect of TR choice on image contrast can be seen in Figure 13. The signal from stationary material is less suppressed with increasing TRs. The high contrast from unsaturated magnetization in newly arriving flowing nuclei is retained longer with longer TRs. However, the total acquisition time increases with increasing TRs. Again, a compromise must be made.

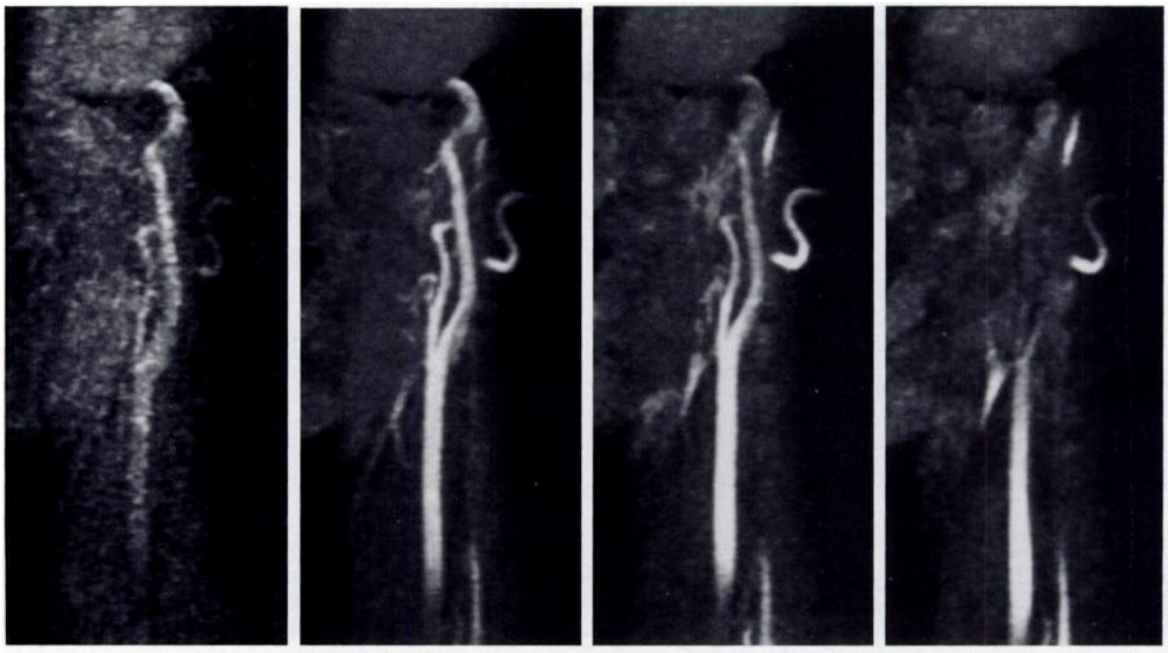

12a. 12b. 12c. 12d.

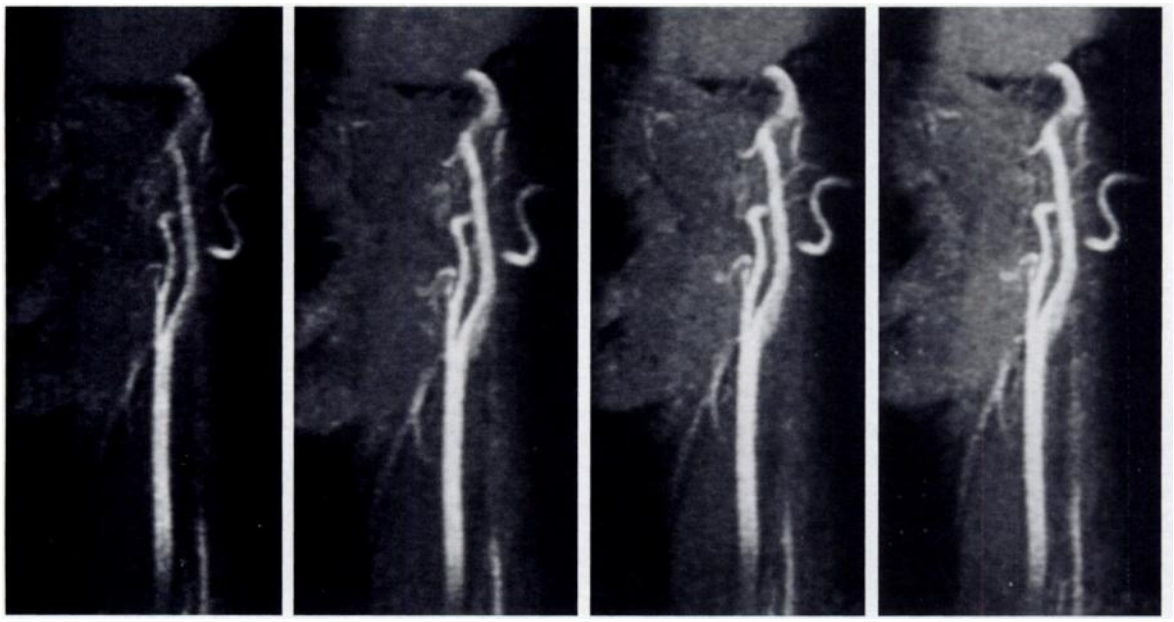

13a. 13b. 13c. 13d.

Figures 12, 13. **(12)** Lateral MIP MR angiograms demonstrate the dependence of contrast on flip angle. Images were constructed from three-dimensional sagittal data acquisitions (30/7, 40-mm-thick slab, 32 partitions) of the carotid bifurcation with flip angles of 5° **(a)**, 20° **(b)**, 35° **(c)**, and 50° **(d)**. Optimal signal is seen in the image obtained with a 20° flip angle **(b)**. **(13)** Lateral MIP MR angiograms demonstrate the dependence of contrast on TR. Images were constructed from three-dimensional sagittal data acquisitions (7-msec TE, 30° flip angle, 40-mm-thick slab, 32 partitions) of the carotid bifurcation with TRs of 20 msec **(a)**, 40 msec **(b)**, 60 msec **(c)**, and 80 msec **(d)**. Increased vascular signal is seen with increasing TR, but this results in reduced saturation of stationary tissue.

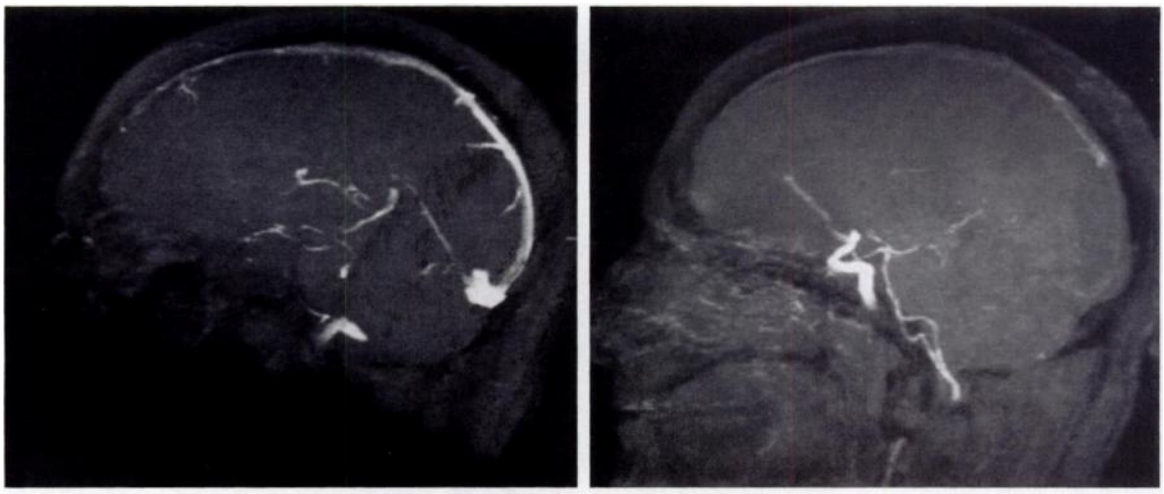

a. b.

Figure 14. Lateral MIP MR angiograms obtained with sequential two-dimensional **(a)** and true three-dimensional **(b)** data acquisitions demonstrate the dependence of the imaging technique on flow velocity. Slow-flowing blood in the sagittal sinus is much better appreciated on the two-dimensional image **(a)**. (The two-dimensional acquisition included an inferior saturation band that removed the arterial signal.)

■ SATURATION

The specific rate of signal loss as one progresses distally along a vessel depends on the time that nuclei have remained within the excitation volume and thus depends sensitively on the flow velocities. This effect can be seen in a comparison of sequential two- and three-dimensional MR angiographic studies through the brain and their depictions of the sagittal sinus (Fig 14). In the sequential two-dimensional study, a series of 36 parasagittal sections rotated from sagittal to coronal were collected. Each section was 4 mm thick. This permitted good inflow replenishment into each section, and the sagittal sinus was well visualized. In the three-dimensional study, a 32-mm-thick sagittal slab was excited. The slow-flowing venous blood in the sagittal sinus remained within the excitation volume, and no significant inflow replenishment was possible, resulting in poor visualization of the sagittal sinus.

■ MOTION COMPENSATION

Conventional GRE sequences result in inconsistent flow signal and pronounced intravascular signal loss (10). It was only after methods were developed that corrected for signal loss associated with motion that MR angiographic studies were feasible (11).

MR section-selective gradients and spatial-encoding gradients are designed to bring all excited nuclei (which are aligned along the same direction in space) back into alignment at the center of the signal readout period, thus generating an echo. The relevant mechanisms are discussed herein with reference to the frequency-encoding gradient. Gradient waveforms first dephase the nuclei by a certain amount. The dephasing gradient is followed by a rephasing gradient. In the interval during which the rephasing gradient is applied, signal is also measured. The signal peak, the echo, occurs when the effect of the rephasing gradient cancels the effect of the dephasing gradient and the nuclei return to their initial alignment. This happens at the same time for all stationary nuclei, indepen-

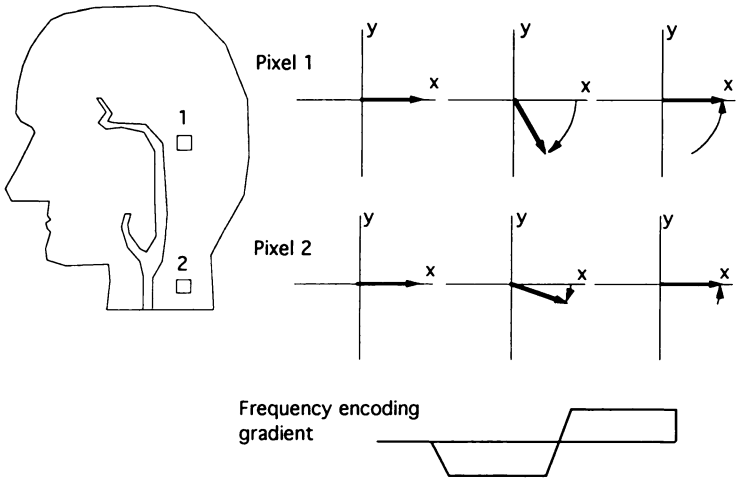

Figure 15. Diagram depicts the effect of dephasing and rephasing gradients on stationary nuclei. After RF excitation, all nuclei are aligned along the same direction in space. Frequency-encoding gradients are designed to first dephase nuclei and then bring all transverse magnetization back into alignment at the center of the signal readout period (the echo).

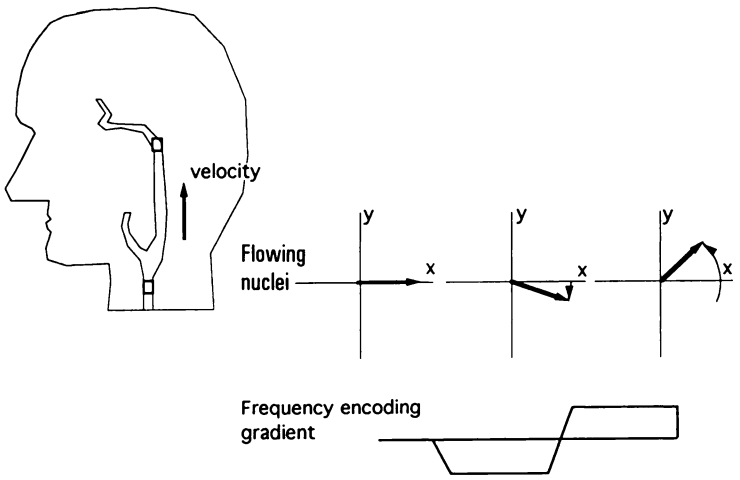

Figure 16. Diagram depicts the effect of dephasing and rephasing gradients on moving nuclei. Because of their motion, individual moving nuclei experience dephasing and rephasing gradients of different magnitude, placing the nuclei out of alignment at the center of the signal readout period.

dent of their location (Fig 15). Nuclei in a low strength field undergo little dephasing and rephasing. Nuclei in a high strength field are dephased to a great extent but are rephased by an equal amount. Nuclei at both locations are aligned at the center of the echo.

Moving nuclei may be located in a region of low gradient strength when the dephasing gradient is applied, and they will be dephased by a small amount. However, when the rephasing gradient is applied, they will have moved to a region with higher gradient strength and the amount of rephasing that they receive will overcompensate for the dephasing, placing them out of alignment at the center of signal acquisition (Fig 16).

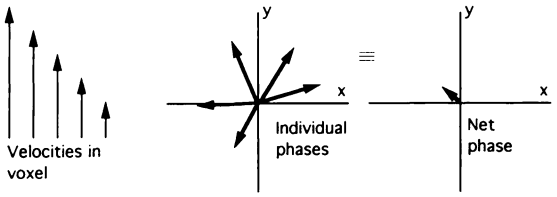

Figure 17. Diagram depicts the variable dephasing of nuclei with different velocities within a single voxel. Nuclei misalignment depends on velocity, resulting in a reduction of intravoxel signal, referred to as intravoxel phase dispersion.

The extent to which the moving nuclei are misaligned at the center of the readout period will depend on their displacement through the encoding gradients. The faster the nuclei move, the greater the misalignment. Within any single voxel, there is generally a spread of flow velocities and hence a spread of misalignment. The end result is that the net transverse magnetization in the voxel is substantially decreased—an effect referred to as intravoxel phase dispersion (Fig 17). The extent of intravoxel phase dispersion at any given phase-encoding step will vary with pulsatile flow and result in signal mismapping and image artifacts.

It is possible to bring all nuclei moving with constant velocity back into alignment at the center of signal readout by using more complicated gradient waveforms. These waveforms typically consist of three lobes of gradient strength (Fig 18); however, they will not correct for higher-order motion such as acceleration. Each axis must be independently accounted for, and flow compensation gradients are conventionally applied along the section-select and frequency-encoding axes.

A comparison of MR angiograms obtained with and without flow compensation is shown in Figure 19. The arterial signal is correctly mapped within the lumen of the vessel in the velocity-compensated image, whereas it is incoherently "splattered" throughout the image obtained without flow compensation.

Flow compensation methods take into account constant velocity motion and do not correct for the high-order motion that occurs at the origins of vessels and distal to vessel stenoses. In those cases, intravoxel phase dispersion persists and stenosis can be overestimated (Fig 20).

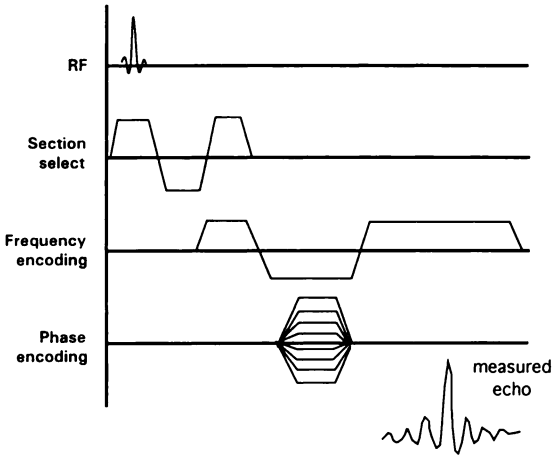

Figure 18. Diagram shows a flow-compensated GRE sequence. All nuclei moving with constant velocity are brought into alignment at the center of the signal readout period by using a three-lobed gradient waveform.

a. **b.**

Figure 19. Coronal single-section MR angiograms through the common carotid artery were acquired without flow compensation **(a)** and with first-order (velocity) flow compensation in the section-select and frequency-encoding directions **(b)**. The arterial signal is correctly depicted in the velocity-compensated image **(b)**.

■ SHORT TE SEQUENCES

With increased gradient strengths and reduced times to reach maximum strength, it is possible to create pulse sequences with shorter TEs that have reduced durations of spatial-encoding gradients. The shorter TE sequences are therefore less sensitive to high-order motion and allow assessment of stenoses that is more similar to evaluation with x-ray angiography. This effect is

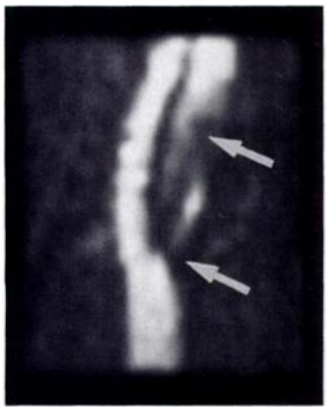

Figure 20. Lateral MIP MR angiogram demonstrates the sensitivity of the technique to complex flow. Image was constructed from sequential axial two-dimensional sections (acquired with a 10-msec TE) through the carotid artery of a patient with critical stenosis. High-order motion leads to intravoxel phase dispersion and regions of total signal loss (arrows), resulting in overestimation of the degree of stenosis.

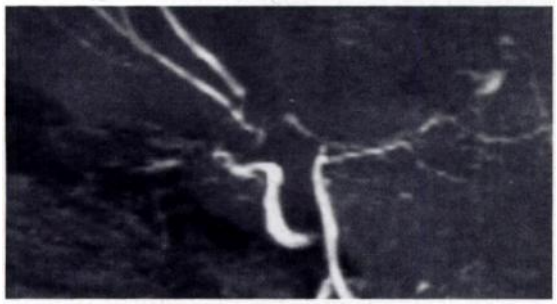

a.

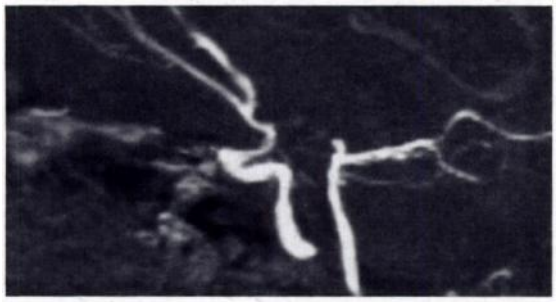

b.

Figure 21. Lateral MIP MR angiograms demonstrate the effect of TE on depiction of flow in tortuous vessels. Images were constructed from three-dimensional acquisitions of the carotid siphon obtained with a 7-msec TE and constant velocity compensation along frequency-encoding and section-select directions **(a)** and with a 5-msec TE and flow compensation along the same axes **(b)**. The image with the longer TE **(a)** is affected much more than the image with the shorter TE **(b)** by the high-order motion that accompanies flow through the tortuous vessel.

very noticeable in studies of the carotid siphon, where there are strong accelerative components because of the tortuous geometry (Fig 21).

■ TWO- VERSUS THREE-DIMENSIONAL TOF MR IMAGING

Both two- and three-dimensional TOF MR angiographic studies have advantages and limitations. The major advantage of two-dimensional methods is that blood flowing into the excitation volume need replenish only a thin volume of material to provide high flow signal. Because of this reduced sensitivity to saturation effects, two-dimensional methods are indispensable for the evaluation of slow-flow states and, in particular, for differentiating between slow flow and occlusion. Two-dimensional methods often use larger flip angles because there is less effect from saturation, and better suppression of signal from stationary nuclei can be achieved. In two-dimensional imaging, thinner sections must be excited, which requires increased gradient strengths and gradient durations, resulting in greater artifactual signal loss from high-order motion than occurs in three-dimensional imaging.

Whereas in-plane saturation can be fairly substantial in two-dimensional methods, the small flip angles used in three-dimensional methods make them relatively independent of flow direction and more useful in imaging tortuous vessels. Three-dimensional methods also provide absolutely contiguous sections with little intravoxel phase dispersion because of the smaller voxels that can be achieved and the shorter duration gradient times that are used. Finally, three-dimensional methods benefit from the inherently better resolution that they possess and a significant reduction in partial volume averaging.

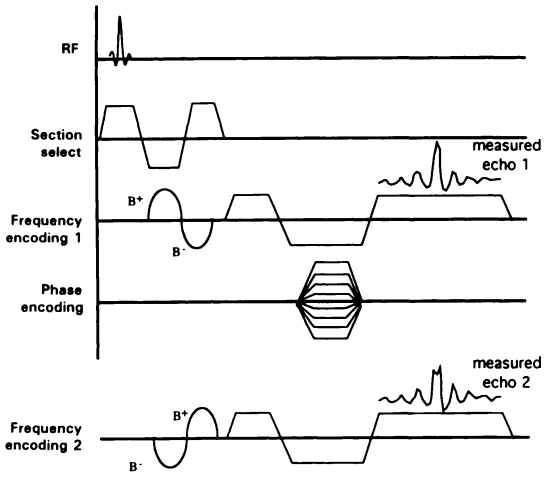

Figure 22. Diagram of a two-dimensional phase-contrast pulse sequence. An additional bipolar lobe (B^- and B^+) of encoding gradient is applied in each image acquisition but with reversed polarity (shown here for the frequency-encoding axis). The two images are then subtracted.

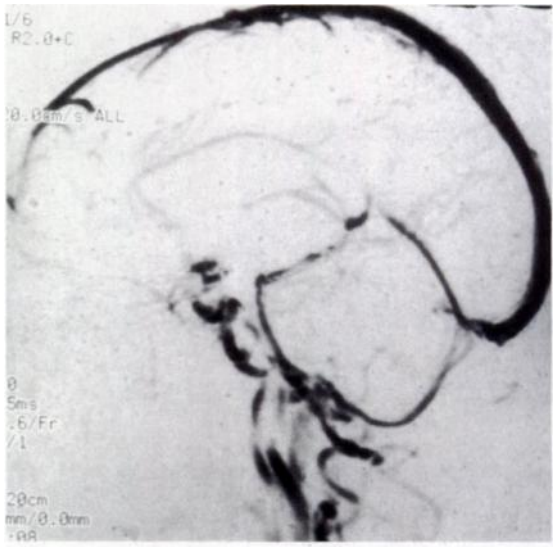

Figure 23. "Speed" image of the head constructed from a two-dimensional sagittal phase-contrast MR angiographic acquisition performed with 25/15, 50-mm section thickness, and velocity-encoding strength of the gradients of 20 cm/sec. To improve signal-to-noise ratio, 16 signal averages were performed.

■ PHASE-CONTRAST ANGIOGRAPHY

Phase-contrast angiography generates signal contrast between flowing and stationary nuclei by sensitizing the phase of the transverse magnetization to the velocity of motion. Two data sets are acquired with opposite sensitization, yielding opposite phase for moving nuclei and identical phase for stationary nuclei (12). When the two data sets are subtracted, signal contribution from stationary nuclei is eliminated and only flowing nuclei are seen. Because this signal is eliminated, the two data sets can be acquired in projection through a thick two-dimensional slab. They can also be collected as true three-dimensional data sets. Studies in which images of the same section are acquired at multiple points in the cardiac cycle, called cine studies, can provide interesting information on flow dynamics.

To appropriately sensitize the nuclei to velocity, a bipolar lobe of encoding gradient is applied in each image acquisition but with reversed polarity. Each encoding axis must be sensitized to account for velocity components along all axes. Figure 22 illustrates the different gradient waveforms that would be applied along the frequency-encoding axis. Saturation effects are less important in phase-contrast studies than in TOF studies because even heavily saturated nuclei will generate a phase angle substantially larger than that of stationary nuclei.

Because TOF studies display the magnitude of the magnetization, the absolute value of the phase shift within each voxel is not important (provided there is no intravoxel phase dispersion). The net phase accumulation within a voxel is, however, a key consideration when a phase-contrast study is planned. The pulse sequences used in phase-contrast studies are designed to impart a phase shift to nuclei that is proportional to the velocity of the nuclei. The measured phase is determined within a range from -180° to 180°. If a nucleus is moving such that the accumulated phase lies outside this range, the phase will be incorrectly interpreted—an effect referred to as aliasing (similar to the wraparound artifact seen in MR images or the aliasing artifact seen in Doppler sonograms). The acquired phase shift for a moving nucleus is a product of the velocity of the moving nucleus, the gradient strength, and the interval between gradient-encoding lobes. The gradient strength and timing can thus be designed to impart a maximal phase shift (±180°) for a given velocity. The parameter in the pulse sequence that determines the velocity above which aliasing occurs (referred to as the velocity encoding level [VENC]) must therefore be chosen with a value appropriate to the anticipated flow velocities in the vasculature of interest.

The application of a two-dimensional phase-contrast method for imaging the relatively slow flow in the head is shown in Figure 23. The slow flow in the sagittal sinus is well visualized with the pulse sequence used.

To derive a true three-dimensional data set, three-dimensional phase-contrast angiograms can be acquired. These data sets have smaller

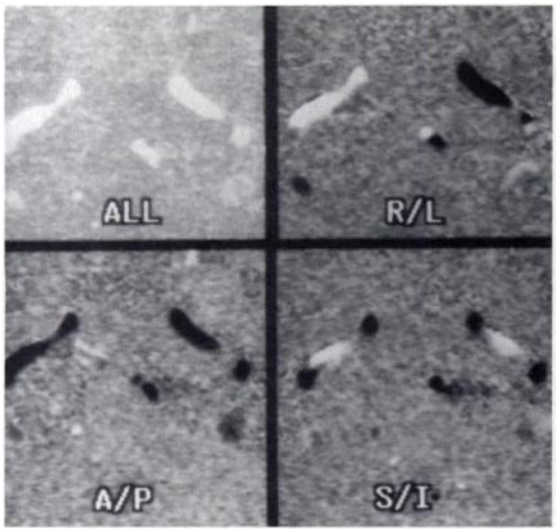

Figure 24. Four images from a three-dimensional phase-contrast study of the circle of Willis. The summed information from all three flow directions is represented in the speed image (top left), and flow directionality along the three gradient axes—right-left (*R/L*), anterior-posterior (*A/P*), and superior-inferior (*S/I*)—is shown in the top right, bottom left, and bottom right images, respectively.

voxels and therefore better resolution. They also provide information on flow directionality along each of the three encoding axes: right-left, anterior-posterior, and superior-inferior (Fig 24). Furthermore, the summed information from all three flow directions is represented in the speed image, in which the signal intensity is proportional to the magnitude of the flow velocity. The data acquisition requires four measurements—one for each encoding direction and one reference set—and is therefore relatively lengthy.

Phase-contrast MR angiography can be effectively used to avoid problems of magnetization saturation that occur in three-dimensional TOF studies. The phase-contrast techniques are also useful in eliminating signal from high-intensity stationary material such as blood products, which, because of their very short T1 values, may appear bright and mimic flow signal in TOF studies. The major drawbacks of phase-contrast methods are the relatively lengthy acquisition times that are needed and the need to match the imaging gradient sensitivity to the anticipated flow conditions a priori. Inappropriate settings can lead to aliasing effects in which flow directionality is incorrectly displayed or to reduced sensitivity. Phase-contrast methods also impose strong demands on magnetic field gradient performance.

■ CONCLUSION

MR angiography is an attractive modality for the noninvasive evaluation of vascular disease. It holds the potential for providing information on vascular pathologic conditions and for determining the hemodynamic implications of vascular disease. Together with MR imaging methods to evaluate the end organ, it is a powerful technique for the clinical evaluation of vascular disease.

■ REFERENCES

1. Haacke EM, Masaryk TJ. The salient features of MR angiography. Radiology 1989; 173:611-612.
2. Listerud J. First principles of magnetic resonance angiography. Magn Reson Q 1991; 7: 136-170.
3. Haacke EM, Lin WL. Technologic advances in magnetic resonance angiography. Curr Opin Radiol 1991; 3:240-247.
4. Potchen E, Haacke E, Siebert J, Gottschalk A. Magnetic resonance angiography. St Louis, Mo: Mosby, 1993.
5. Anderson C, Edelman R, Turski P. Clinical magnetic resonance angiography. New York, NY: Raven, 1993.
6. Rossnick S, Laub G, Braeckle R. Three dimensional display of blood vessels in MRI. In: Proceedings of the IEEE Computers in Cardiology. New York, NY: Institute of Electrical and Electronic Engineers, 1986; 193-195.
7. Edelman RR, Mattle HP, O'Reilly GV, Wentz KU, Liu C, Zhao B. Magnetic resonance imaging of flow dynamics in the circle of Willis. Stroke 1990; 21:56-65.
8. Schmalbrock P, Yuan C, Chakeres DW, Kohli J, Pelc NJ. Volume MR angiography: methods to achieve very short echo times. Radiology 1990; 175:861-865.
9. Alfidi RJ, Masaryk TJ, Haacke EM, et al. MR angiography of peripheral, carotid, and coronary arteries. AJR 1987; 149:1097-1109.
10. von Schulthess G, Higgins C. Blood flow imaging with MR: spin-phase phenomena. Radiology 1985; 157:687-695.
11. Pattany M, Phillips J, Chiu L, et al. Motion artifact suppression technique (MAST) for MR imaging. J Comput Assist Tomogr 1987; 11: 369-377.
12. Dumoulin CL, Yucel EK, Vock P, et al. Two- and three-dimensional phase contrast MR angiography of the abdomen. J Comput Assist Tomogr 1990; 14:779-784.

This article meets the criteria for 1.0 credit hour in Category 1 of the AMA Physician's Recognition Award. To obtain credit, see questionnaire on pp 439-432.